Hindawi
International Journal of Polymer Science
Volume 2019, Article ID 4740765, 10 pages
https://doi.org/10.1155/2019/4740765

Research Article

Silk Sericin Semi-interpenetrating Network Hydrogels Based on PEG-Diacrylate for Wound Healing Treatment

Patchara Punyamoonwongsa,[1] **Supattra Klayya**,[1] **Warayuth Sajomsang**,[2] **Chanikarn Kunyanee**,[3] **and Sasitorn Aueviriyavit**[3]

[1]*School of Science, Mae Fah Luang University, Muang, Chiang Rai 57100, Thailand*
[2]*Nanoengineered Soft Materials for Green Environment Laboratory, National Nanotechnology Center, Pathum Thani 12120, Thailand*
[3]*Nano Safety and Risk Assessment Laboratory, National Nanotechnology Center, Pathum Thani 12120, Thailand*

Correspondence should be addressed to Patchara Punyamoonwongsa; patchara@mfu.ac.th

Received 15 February 2019; Revised 1 August 2019; Accepted 28 August 2019; Published 28 October 2019

Academic Editor: Miriam H. Rafailovich

Silk sericin (SS) from the *Bombyx mori* silk cocoons has received much attention from biomedical scientists due to its outstanding properties, such as antioxidant, antibacterial, UV-resistant, and ability to release moisturizing factors. Unmodified SS does not self-assemble strongly enough to be used as a hydrogel wound dressing. Therefore, there is a need for suitable stabilization techniques to interlink the SS peptide chains or strengthen their structural cohesion. Here, we reported a method to form a silk semi-interpenetrating network (semi-IPN) structure through reacting with the short-chain poly(ethylene glycol) diacrylate (PEGDA) in the presence of a redox pair. Various hydrogels were prepared in aqueous media at the final SS/PEGDA weight percentages of 8/92, 15/85, and 20/80. Results indicated that all semi-IPN samples underwent a sol-gel transition within 70 min. The equilibrium water content (EWC) for all samples was found to be in the range of 70-80%, depending on the PEGDA content. Both the gelation time and the sol fraction decreased with the increased PEGDA content. This was due to the tightened network structure formed within the hydrogel matrices. Among all hydrogel samples, the 15/85 (SS/PEGDA) hydrogel displayed the maximum compressive strength (0.66 MPa) and strain (7.15%), higher than those of pure PEGDA. This implied a well-balanced molecular interaction within the SS/PEGDA/water systems. Based on the direct and indirect MTS assay, the 15/85 hydrogel showed excellent *in vitro* biocompatibility towards human dermal fibroblasts, representing a promising material for biomedical wound dressing in the future. A formation of a semi-IPN structure has thus proved to be one of the best strategies to extend a practical limit of using SS hydrogels for wound healing treatment or other biomedical hydrogel matrices in the future.

1. Introduction

Hydrogels have received much attention from researchers for the past decades. They are three-dimensional (3D) polymeric networks and resistant to swell in an aqueous solution without losing their structural integrity. They have impressively high degree of water content, thus mimicking some tissues and extracellular matrices (ECM) [1]. Hydrogel biomaterials, including as drug delivery systems, biosensors, contact lenses, immobilization carriers, and matrices for tissue engineering technology, have already been reported [2–4]. One of many advantages of hydrogels is a great variety of methods to establish the crosslinking within the polymer matrices. Generally, hydrogel networks can be formed by either a chemical or a physical method [5]. The physically crosslinked hydrogels are formed by molecular entanglements, ionic attraction, hydrogen bonding, and hydrophobic forces. The chemical crosslinking hydrogels are usually obtained by forming a covalent bond between the polymeric chains through a redox, photo-, or thermal polymerization reaction. Physical gels are of interest for both biomedical and cosmetic applications due to their excellent biocompatibility [2, 6]. Despite this, they are too weak to be processed into a membrane sheet format. This is because their networks

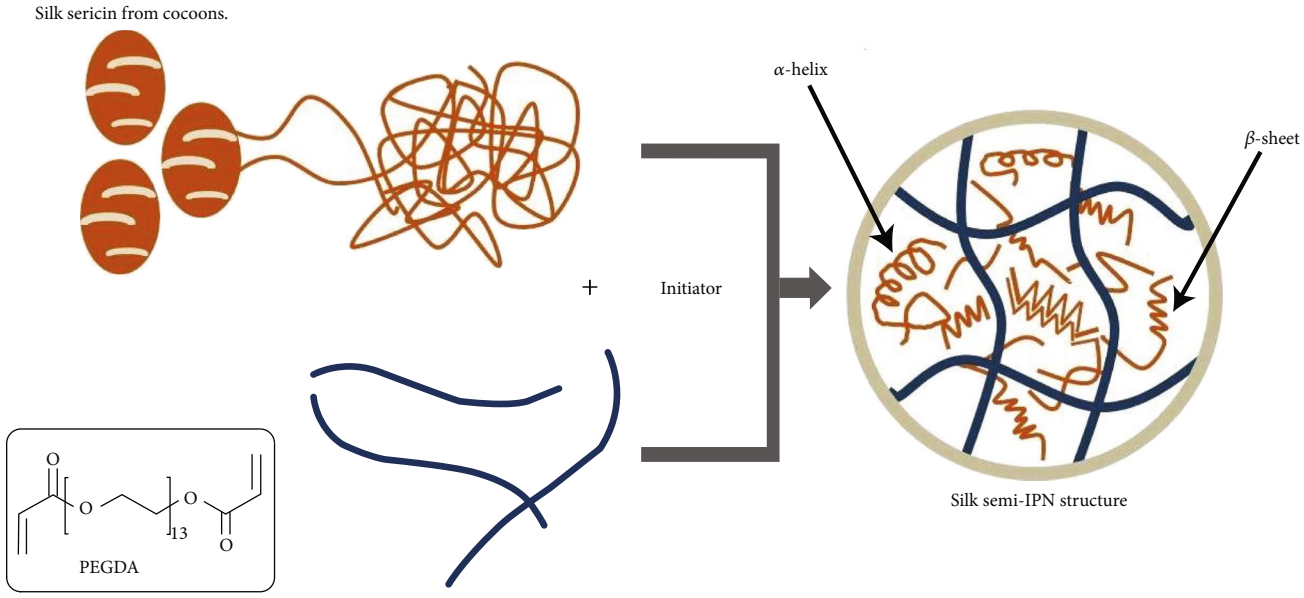

Figure 1: Schematic illustration of the formation of a SS/PEGDA semi-IPN hydrogel network.

are simply held by molecular entanglement and/or dispersive forces [7]. Moreover, a physically crosslinked network is uncontrollable, inhomogeneous, and destabilized quite easily in aqueous media. Chemically crosslinked hydrogels are more reproducible, tunable, and display excellent structural cohesion [6, 8, 9]. However, due to nonphysiological conditions employed, chemical crosslinking may provoke tissue reaction, immunological response, and cytotoxic effects. Beside the preparation method, the sources of raw materials also affect their biological properties. For example, hydrogels from natural polymers, such as polysaccharides and proteins, usually display greater biocompatibility, comparing to synthetic polymers. This could be attributed to their ability to be metabolized into harmless products or excreted by a renal filtration process [6]. However, the uses of natural proteins are often restricted due to their potential immunogenic reactions and relatively poor mechanical properties [10].

Silk fiber is a protein-based material made by arthropods for a variety of task-specific purposes. It can be found in different chemical compositions, structural conformations, and physicochemical properties, depending on the original sources [3, 11]. The most extensively characterized silk fibers are from the domesticated *Bombyx mori* silkworm. Silk fiber by cultivated *Bombyx mori* silkworm is mainly consisted of the two proteins: sericin (20-30%) and fibroin (70-80%) [11]. While the fibrous silk fibroin (SF) protein contributes to the fiber strength, the silk sericin (SS) protein takes a major role on binding the two SF filaments together. Due to higher content of polar amino acids, SS can easily be dissolved in alkaline solution, yielding a yellowish solution called regenerated SS (RSS) solution [12, 13]. RSS has already been applied as hydrogel matrices for biological sensors, enzyme immobilization, tissue engineering scaffolds, and wound dressing. Hydrogels of SS showed excellent properties, such as good adhesiveness, biocompatibility, antioxidant and antibacterial activity, UV-resistant, and good moisturizing effects to the skin [4, 13]. Nonetheless, physical SS gels normally exhibit poor water resistance with low mechanical properties, thus limiting their use in practice. To resolve this issue, a formation of interpenetrating networks (IPNs) was suggested [4, 8, 14–16]. IPNs are crosslinked polymers, in which at least one network is crosslinked in the presence of another one. They can be either full- or semi-IPN types. In semi-IPN, one of the constituent forms the 3D network, while the linear chains of another constituent are physically interacted among themselves and with the 3D network [15]. This network formation helps to stabilize the hydrogel structure, making them more suitable for a wider context of biomedical applications.

Silk fibroin semi-IPN hydrogels based on poly(ethylene glycol) diacrylate (PEGDA, MW 700), a chemical structure shown in Figure 1, were reported earlier [8]. Many hydrogel properties, such as water resistance, gelation kinetics, water content, and release character, were improved by PEGDA alteration. With the increased PEGDA, the tightened network structure could stabilize the hydrogels in aqueous media and facilitate diffusion hindrance to deliver the model compound (rhodamine B) over a prolonged period of time. PEGDA is a well-known homobifunctional crosslinker to reinforce many naturally derived hydrogel matrices. Incorporation of PEGDA segments was reported to promote cell encapsulation and migration [17, 18]. Over time, they could partially be biodegraded via hydrolytic degradation [19]. To the best of our knowledge, semi-IPN SS/PEGDA hydrogel has never been reported. A combined favorable property of each component could potentially lead to a new hydrogel wound dressing with improved mechanical properties, water resistance, and predictable gelation kinetics, while maintaining their biocompatibility and biodegradability over a period of time. This study demonstrated a way to stabilize SS hydrogels by forming a semi-IPN based on the PEGDA network. The new hybrid hydrogels were synthesized by the chain-growth polymerization mechanism, using ammonium persulfate (APS) and ascorbic acid (AA) as the redox

initiation system. The use of APS in different water-based polymerization systems had already been reported for biomedical applications [20–23]. To study the effect of the feed composition on the gelation time and swelling behaviour, PEGDA content was varied from 80 to 100% (*w*/*w*). The resultant hydrogels were characterized in terms of their structural component, mechanical properties, morphological detail, and *in vitro* cytotoxicity.

2. Materials and Methods

2.1. Materials. *Bombyx mori* silk cocoons were supplied from Silk Innovation Center, Mahasarakham University, Thailand. Ammonium persulfate (APS), ascorbic acid (AA), sodium carbonate, PEGDA (MW 700 g/mol, density = 1.12 g/mL), and all other chemicals were obtained from Sigma (USA). Cellulose dialysis membrane (MWCO 3500) was purchased from Pierce (USA).

2.2. Experimental Methods

2.2.1. Preparation of Regenerated Silk Sericin (RSS). The silk cocoons (1.5 g) were cut into small pieces and degummed in a 100 mL of sodium carbonate solution (0.02 M). The solution was dialysed against deionized water for 3 days and freeze-dried (-40°C) to obtain RSS powder.

2.2.2. Preparation of Semi-IPN Hydrogels. SS (0-20% *w*/*w*), APS (40 mg), AA (40 mg), and PEGDA (450 mg) were mixed in deionized water. The mixture was injected into a spherical silicone rubber moulding (10 mm diameter, 1.5 mm thickness) and allowed to gel at room temperature. The samples were removed from the mould, washed, and immersed in deionized water for 24 hr. The initial feed compositions are shown in Table 1.

2.2.3. Rheometry. Dynamic rheological measurement of the gelation process was made with a Bohlin Gemini AR200HR Rheometer equipped with a cone and plate geometry (cone angle 2°, diameter 40 mm). A 2 mL of the reaction mixture was poured onto the lower plate of a rheometer for each determination. The gelation kinetic determination was performed at 25°C, a frequency of 1 rad/s and shear stress of 0.1 Pa to ensure a linear regime of oscillatory deformation. Mineral oil was applied to the edges of the cone to prevent dehydration during the experiments.

2.2.4. Hydrogel Characterization. All infrared spectra (IR) were recorded in the range of 400-4000 cm^{-1} using the accumulation of 32 scans and a resolution of 4 cm^{-1}. To examine the equilibrium water content (EWC), the gel samples were allowed to swell and equilibrated in deionized water for 72 hr to ensure complete equilibration. The swollen gels were withdrawn from the water, and the excess surface water was removed by blotting gently with a filter paper. The weight of the swollen gels was recorded (M_e), before drying in a hot-air oven maintained at 60°C for 72 hr. After that, the dried gels were reweighed (M_0). The EWC value was determined by using equation (1) [12]. For the calculation of the sol fraction, the dry weight of the freshly prepared samples, W_d(sol + gel), was recorded. The samples were then swollen in deionized water at room temperature for 72 hr. After that, the samples were removed and completely redried at 60°C. Their weights were recorded (W_{rd}), and a sol fraction (% Sol) was finally determined by using equation (2) [15]. To compare the compressive properties among different samples, the swollen hydrogels were tested at 25°C and 65% relative humidity. The maximum load and a compression rate were set at 500 N and 1 mm/min, respectively. The surface and interior morphology of the freeze-dried samples were observed by using a scanning electron microscope (SEM). Images were acquired after gold sputtering at an operating voltage and a working distance of 10 kV and 15 mm, respectively.

Table 1: Initial feed compositions of different SS hydrogel samples.

Sample	SS (mg)	APS (mg)	AA (mg)	PEGDA (mg)	SS/PEGDA weight ratio
PEGDA	0	40	40	450	0/100
SS8PEG92	40	40	40	450	8/92
SS15PEG85	80	40	40	450	15/85
SS20PEG80	120	40	40	450	20/80
SS	120	40	40	0	100/0

$$\mathrm{EWC} = \frac{(M_e - M_0)}{M_e} \times 100, \quad (1)$$

$$\%\mathrm{Sol} = \frac{(W_d - W_{rd})}{W_d} \times 100. \quad (2)$$

X-ray diffraction (XRD) patterns of freeze-dried samples were obtained by using a PANalytical X-Pert PRO X-ray generator with Cu K_α radiation ($\lambda = 1.5418$ Å). The X-ray source was operated at 40 kV and 30 mA in the range of $2\theta = 5$-60°. A differential scanning calorimeter (Mettler Toledo DSC3+) was used to measure the transition temperature of the freeze-dried samples. All measurements were performed under nitrogen atmosphere with a flow rate of 10 mL/min and at a heating rate of 10°C/min. The DSC analysis was carried out in the temperature range from 25°C to 250°C.

2.2.5. Cytotoxicity Testing. Hydrogel compatibility was assessed by direct and indirect methods [24]. Human primary dermal fibroblasts (PCS-201-012™, ATCC) at a density of 30,000 cells/well were seeded and cultured in DMEM for 24 hr (24-well plates). In a direct method, the casted hydrogels were transferred into each of the well to allow cellular contact. The agar gel (5% *w*/*w*) was used as a negative control. For an indirect method, freshly prepared hydrogels were extracted in DMEM at 37°C for 72 hr accordingly to the ISO10993-12. After centrifugation at 1300 rpm (5 min), a 0.6 mL of the extracted medium was transferred into each well. The 10% DMSO was used as a positive control in this section. Cell viability was assessed after 24 hr and 48 hr by using the MTS assay (CellTiter 96®, Promega). For this, either hydrogels or extracted mediums were removed. Then,

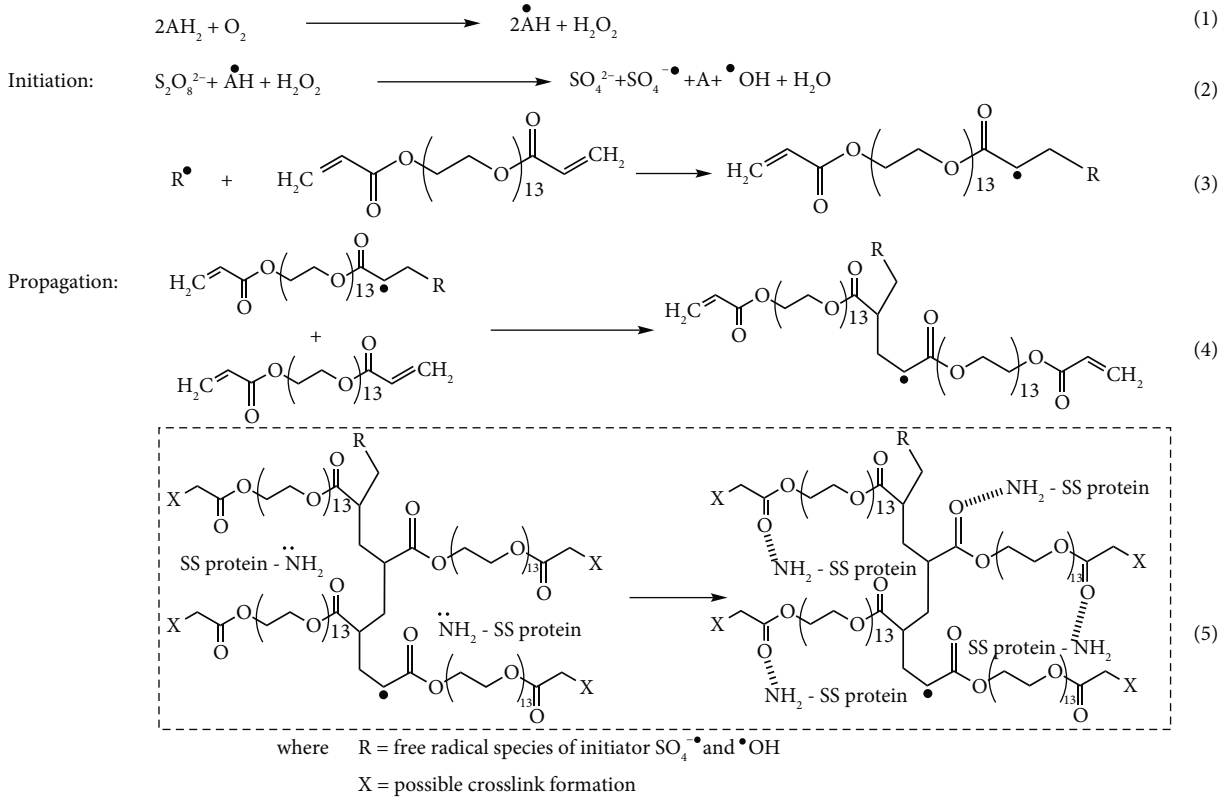

Scheme 1: The reaction mechanism for the formation of silk semi-IPN hydrogels [8].

the cells were washed with PBS and replaced with 400 μL of MTS solution (10-fold diluted in a medium). After 2 hr of incubation at 37°C, the formazan formation reflecting cell viability was measured by using a microplate reader at the absorbance of 490 nm. The untreated control cells (referred to as control cells) were also measured for comparison.

3. Results and Discussion

3.1. Characterization of Hydrogels. Silk sericin (SS) has two main structural conformations, termed α-helix (or random coil) and β-sheet structure. The α-helix coil is an amorphous water soluble (sol) format, while the β-sheet structure is a strong water insoluble format gel. Generally, the silk α-helix coil can be converted to a β-pleated sheet by the alteration of the molecular interactions, such as hydrophobic association, hydrogen bonding, and electrostatic forces [25]. This structural transition transforms the protein from the weak liquid-like (sol) state to the stronger solid-like (gel) state. The process, known as a sol-gel or α-to-β transition, is influenced by temperature, pH solution, ionic strength, and silk concentration [5, 11, 25]. It plays an important role on the network formation within silk gels. Unmodified SS gels normally have unpredictable gelation times. The incorporation of a semi-IPN throughout the SS matrices may help to resolve this problem. To evaluate this, various silk semi-IPN hydrogels were prepared at different SS/PEGDA mass ratios in the presence of an APS/AA redox pair. In oxygen atmosphere, the ascorbate free radical ($A^{\bullet}H$) was believed to catalyze a decomposition of persulfate ($S_2O_8^{2-}$), yielding the primary free radicals ($SO_4^{-\bullet}$, $HO^{\bullet}$) to initiate radical polymerization of PEGDA (Scheme 1). A chain growth of this macromer would eventually lead to a formation of an interconnected 3D structure that physically interacts with the SS chains, thus producing stable semi-IPN, proposed in Figure 1.

To follow the silk gelation kinetics, a dynamic oscillatory rheology was employed. In this study, the storage (G') and loss (G'') moduli were monitored during the *in situ* crosslinking of semi-IPN in the presence of the APS/AA redox initiation system. Isothermal time dependent of G' and G'' for PEGDA and the selected SS/PEGDA samples is illustrated in Figure 2. As noticed, both G' and G'' are quite low at the beginning ($t < t_{gel}$). The fact that G' is less than G'' indicates that in this stage, the system exhibits the characteristics of a viscous fluid. As the gelation proceeded ($t = t_{gel}$), both moduli rapidly increase with the growth rate of G' being higher than that of G''. The difference in the growth rates leads to a crossover of G' and G'', which is defined as the gelation time (t_{gel}), indicating a sol-gel transition of the sample from a viscoelastic liquid to an insoluble elastic gel. The t_{gel} is also referred to as a point at which there is a formation of the semi-IPN through physical and chemical crosslinking.

As noticed in Figure 2 and Table 2, the addition of SS prolongs the PEGDA gelation kinetics. This could be related to the ability of SS to competitively react with the primary radical via tyrosine oxidation, yielding different yellow

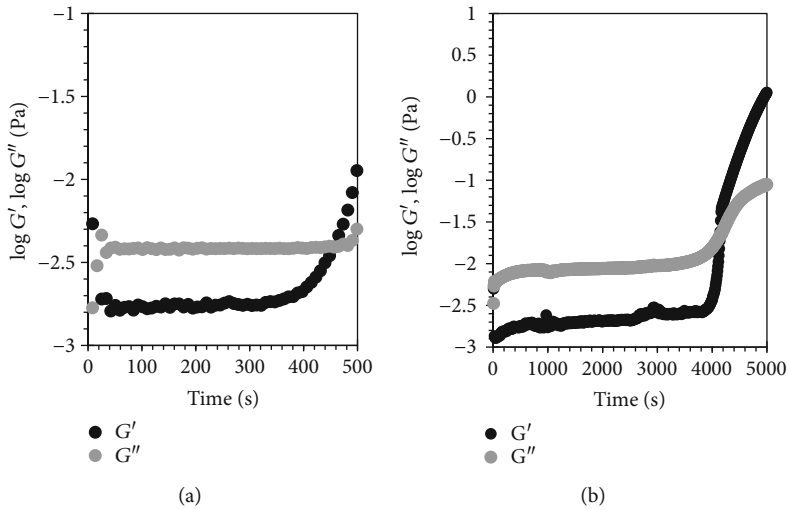

Figure 2: Time evolution of storage modulus (G') and loss modulus (G'') of (a) PEGDA and (b) SS15PEG85 during their gelation at 25°C. The time where G' and G'' crossover is denoted as t_{gel} (gelation time).

Table 2: Various properties of the hydrogel samples.

Sample	Weight percentage of SS/PEGDA	EWC (%)	Sol (%)	Gelation time (min)	Compressive properties	
					Strength (MPa)	Strain (%)
PEGDA	0/100	66.5 ± 2.80	11.7 ± 0.78	8	0.53 ± 0.07	2.63 ± 0.07
SS8PEG92	8/92	70.4 ± 0.84	12.9 ± 0.19	47	0.44 ± 0.07	6.28 ± 0.07
SS15PEG85	15/85	76.2 ± 0.95	15.8 ± 0.31	70	0.66 ± 0.06	7.15 ± 0.08
SS20PEG80	20/80	80.1 ± 1.10	16.7 ± 3.52	62	0.25 ± 0.07	6.41 ± 0.16
SS	100/0	N/a	N/a	>24 hr	N/a	N/a

chromophores, such as dopaquinone and dopachrome [26]. As such, the proportion of active radical species susceptible for PEGDA polymerization would become less available, leading to a prolonged gelation process with lesser effective crosslinking. Over the whole course of the study, unmodified SS (0.06 g/mL) showed no sign of gelation (>24 hr). All other semi-IPN samples underwent a sol-gel transition within 70 min (Table 2). As the PEGDA mass percentage is increased from 85% to 92%, the gelation time is accelerated by the factor of ~1.5. This is associated with the increased number of acrylate-terminated functional groups acquired for effective crosslinking and so, a formation of the fully developed semi-IPN. Nonetheless, the increased PEGDA/SS proportion also causes an undesirable effect. For example, SS20PEG80 shows the EWC value of around 80% (Table 2). A further addition of another 5% and 12% of PEGDA decreases the EWC values to 76% and 70%, respectively. A logical explanation is due to the reduction in polar amino acids (serine, aspartic acid, and threonine) susceptible for water binding within hydrogel matrices. Another reason could be attributed to the tighter hydrogel networks caused by the increased crosslinking density. SEM analysis of the interior morphology of the freeze-dried SS15PEG85 sample reveals the well-defined interconnected spherical pore architecture with the wide pore size distribution (Figures 3(a) and 3(b)). Such extensive networks and interconnected open pore structure would enable cell infiltration and transportation of the solutes (e.g., water molecules and therapeutic drugs). In contrast, PEGDA displays relatively dense interior morphology without interconnecting channels (Figures 3(c) and 3(d)). This intense network topology would generate diffusion hindrance to suppress permeation of the solutes into the hydrogel network. This explains the least water absorbability of SS8PEG92, comparing to the other silk-containing hydrogels (Table 2).

To evaluate the effect of PEGDA on the water resistance, the sol fraction (%) of different hydrogel samples was calculated. This parameter indicates the proportion of gel (water insoluble) fraction remained after dissolution in aqueous media. The lower the % sol, the greater the water resistance, and so, the more suitable would the material become for wound healing treatment. As seen in Table 2, all silk semi-IPN hydrogels displayed less than 20% sol, confirming the improved structural cohesion of the silk hydrogels by forming a semi-IPN. At 92% PEGDA, the semi-IPN hydrogel displays the lowest % sol value of around 13%. The explanation for this is associated with the strongest swelling-resistant effects and the tightened interior network structure upon radical polymerization of PEGDA. Nonetheless, the excess PEGDA addition in turn reduces the hydrogel water content (Table 2). An optimization of PEGDA feed composition needs to be established for an engineering design of SS-

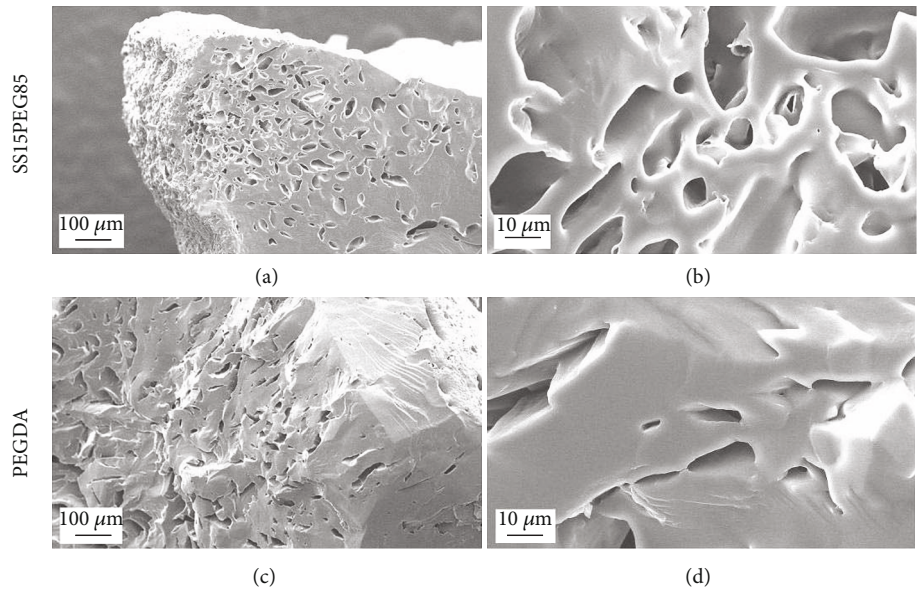

Figure 3: SEM images showing cross-sectional morphology of the freeze-dried hydrogels; SS15PEG85 (a, b) and PEGDA (c, d).

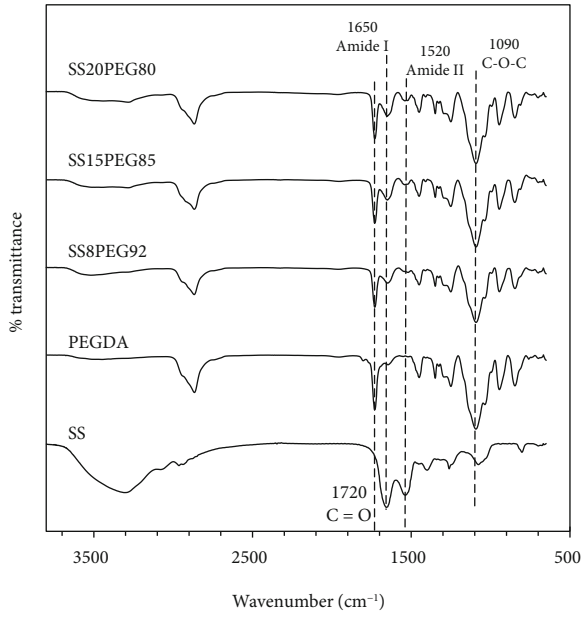

Figure 4: FT-IR spectra of SS raw material, PEGDA hydrogel, and different SS/PEGDA semi-IPN hydrogel samples.

based hydrogels for wound healing and controlled drug delivery applications.

The formation of a primary PEGDA network throughout the hydrogel matrices is proven by the FT-IR technique. As seen in Figure 4, PEGDA hydrogel displays the characteristic IR absorption bands at 1090 cm^{-1} and 1720 cm^{-1}, attributed to the C-O-C and C=O vibrational modes, respectively. The SS raw material shows the characteristic bands at 1650 cm^{-1}(Amide I, C=O stretching) and 1520 cm^{-1} (Amide II, N-H deformation). For all silk semi-IPN samples, the characteristic IR absorption bands of both PEGDA (1090 cm^{-1} and 1720 cm^{-1}) and SS (1520 cm^{-1} and 1650 cm^{-1}) are still detected. This suggests the coexistence of the two components within the silk semi-IPN hydrogels. Due to the overlapped IR bands of the C=C group in PEGDA (1636 cm^{-1}) and the Amide I signal (1650 cm^{-1}), interpretation of the acrylate conversion after crosslinking of PEGDA is therefore limited. For all silk semi-IPN samples, a slight shift of the Amide I signal from 1650 cm^{-1} towards the lower wavenumber regions (1645-1630 cm^{-1}) is observed, implying an occurrence of a silk conformational transition from an α-helical (or random coil) into a β-pleated structure during network formation.

3.2. Mechanical Properties. Hydrogel mechanical strength and strain are one of the very important key factors for biomedical wound dressing. To evaluate these, a compressive mechanical test was employed for different SS/PEGDA semi-IPN samples in their swollen state. The results are shown in Figure 5. Except for the SS15PEG85, the compressive strengths for the hybrid semi-IPN samples are found to be lower than that of pure PEGDA (Figure 5(a)). This may be associated with the enhanced plasticizing effects caused by the nonfreezing water within the hydrogel matrices. The effect, which is known as plasticization or lubrication, normally leads to a reduction of mechanical modulus and the improved material extensibility as in the cases of SS8PEG92 and SS20PEG80 observed in Figure 5(b). Another obvious reason is related to the loosened interior hydrogel networks formed within the 8/92 and 20/80 (SS/PEGDA) hydrogel systems, comparing to pure PEGDA (0/100). Since the formation of stable semi-IPN is primarily governed by the extent of PEGA crosslinking, the reduced PEGDA addition from 8/92 and 20/80 proportions would result in the formation of loosely interconnected semi-IPNs with lowered crosslinking density. Many hydrogel properties, including free volume cavity, chain mobility, glass transition temperature, drug release characters, and ability to withstand applied mechanical stresses, are known to depend on the

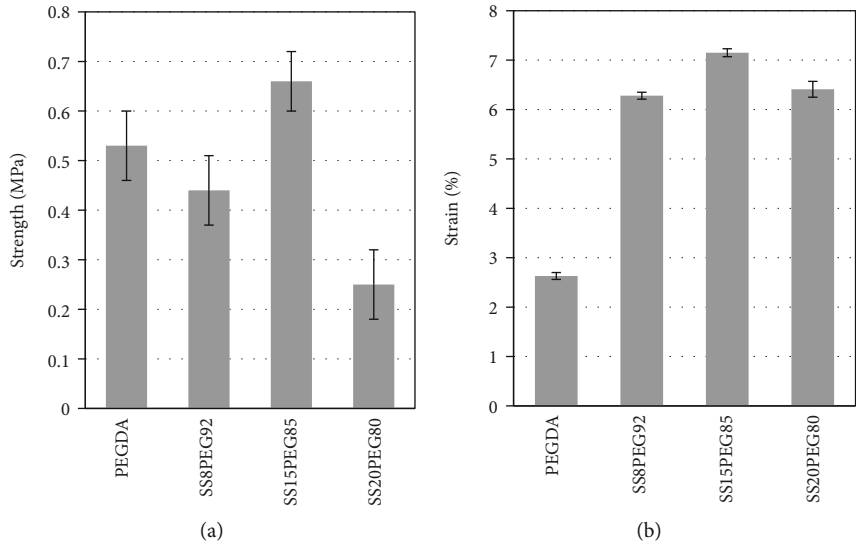

Figure 5: The compressive strength (a) and strain (b) of different hydrogel samples ($n = 3$).

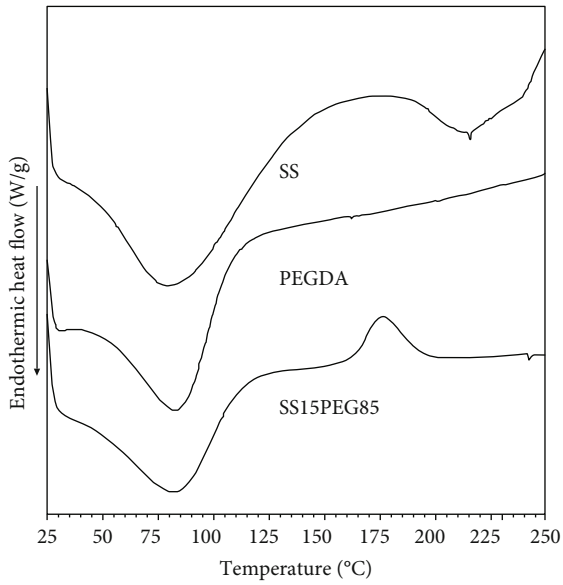

Figure 6: DSC thermograms of different freeze-dried samples.

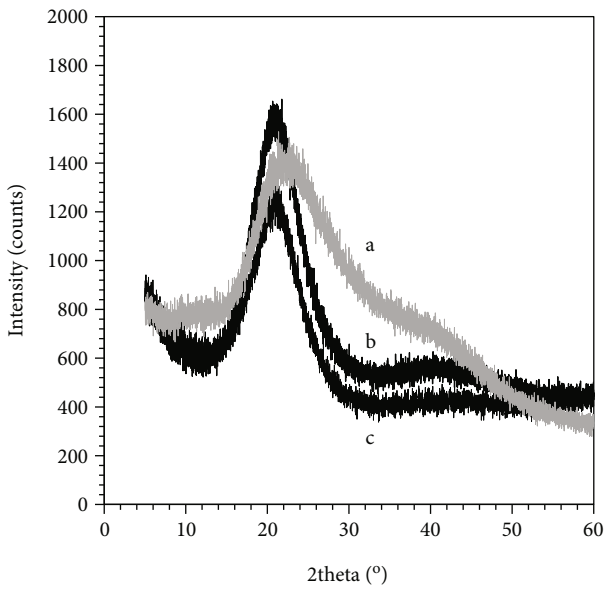

Figure 7: X-ray diffraction of the freeze-dried samples: (a) SS powder, (b) PEGDA hydrogel, and (c) SS15PEG85 hydrogel.

extent of crosslinking. The lower the crosslinking density, the larger the free volume cavity, and so, the faster the diffusion rate of solute molecules throughout hydrogel matrices. However, this in turn weakens the ability of the hydrogel to withstand extensive deformation. This is perhaps the case of SS8PEG92 and SS20PEG80, as observed in Figure 5(a).

The more interesting but yet complicated is observed in the 15/85 hydrogel system (SS15PEG85). As shown in Figure 5(a), this hydrogel shows almost twenty-five percentage increase of the compressive strength comparing to pure PEGDA. The compressive strength of the 15/85 sample has reached to the maximum value of around 0.66 MPa. This could be attributed to the precisely balanced molecular interactions within the SS15PEG85 system. The results from DSC (Figure 6) and XRD (Figure 7) analyses of the freeze-dried SS, PEGDA, and SF15PEG85 samples provide good supportive evidence for this matter. As noticed in Figure 6, the first endothermic peaks observed at 82.17°C (SS), 84.50°C (PEGDA), and 83.00°C (SS15PEG85) are considered to be related to the loss of moisture. No exothermic transition is observed in the DSC curve of PEGDA, suggesting a dense crosslink junction with little or no dangling chain ends. In the DSC curve of SS, the endothermic baseline shift around 198°C, corresponding to the glass transition temperature (T_g), is detected. This value is found to be higher than that reported (175-190°C) [27, 28], implying a constrained segmental motion of the silk amorphous chains caused by partial crystallization. In contrast to SS, the SS15PEG85 displays the exothermic transition at 175°C, lower than that

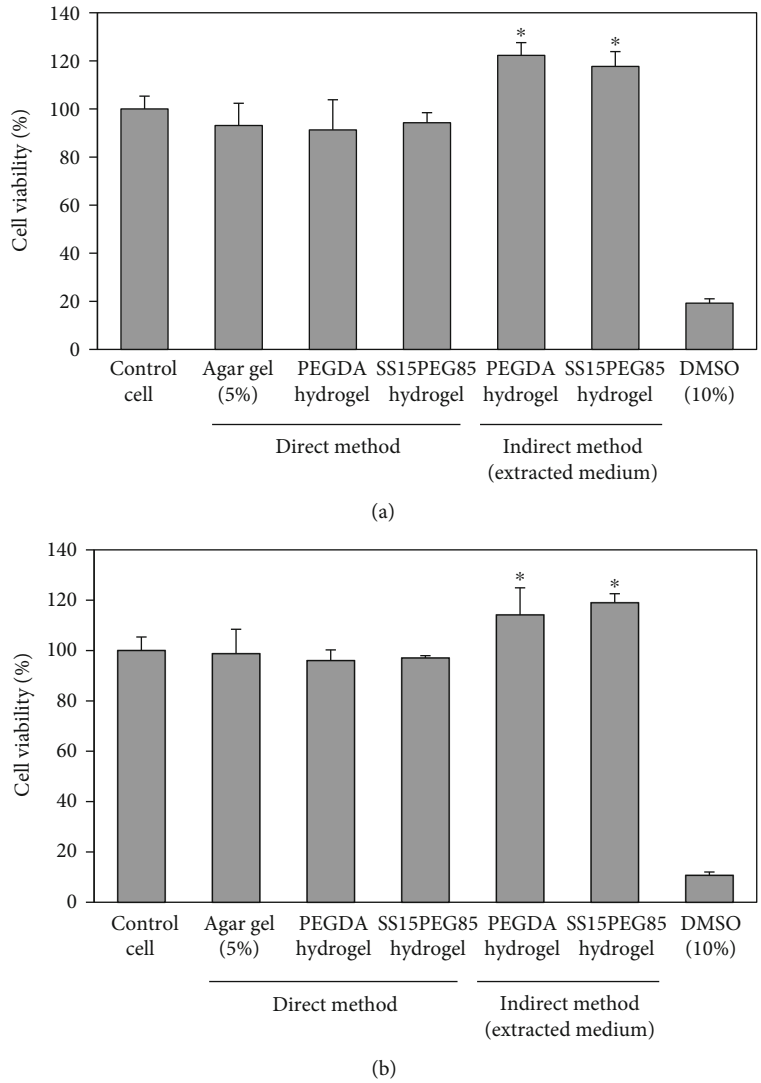

Figure 8: The cell viability by MTS assay using direct and indirect methods ($n = 3$). The dermal fibroblasts were exposed to SS15PEG85 for (a) 24 hr and (b) 48 hr.

reported by Tsukada et al. (205°C) [28]. Due to the preferential molecular interactions within the SS/PEGDA/water systems, the silk recrystallization is believed to be more energetically possible than in sericin itself alone. The silk crystallization (so-called α-to-β phase transition) generally requires the close proximity molecular hydrogen bonds among the peptide chains. In the 15/85 hydrogel system, the process of silk self-aggregation may be accelerated through the action of PEGA inducer. Here, the intermolecular hydrogen bonds within the water-PEGDA system are preferentially stronger than those in the water-SS system. The water molecules around the polypeptide would be then squeezed out, leading to a disruption of the silk hydration sphere. Such reduced water molecules around the peptide chains would allow the molecules of SS to hydrophobically intertwine, agglomerate, and eventually undergo an α-to-β phase transition. The ability of the poly(ethylene glycol) derivatives to act as an inducer of silk phase transition has already been reported earlier [14, 29, 30]. A slightly shift of the Amide I signal observed in Figure 4 also reconfirms the formation of such silk crystallization. Figure 7 displays the XRD patterns of SS, PEGDA, and SS15PEG85 samples. SS exhibits a relatively broad diffraction peak from 18° to 32°, indicating the predominant amorphous nature of the silk protein (Figure 7(a)). For PEGDA and SS15PEG85 hydrogels (Figures 7(b) and 7(c)), the crystalline diffraction peak corresponding to a helix structure of PEGDA is found between 20° and 24° [31], suggesting that the continuous PEGDA chain folding into crystallites is not inhibited by the chain-growth polymerization or the presence of SS compartment. Nonetheless, the broadening in the XRD peak suggests the formation of the nonperfect PEGDA crystals in both gel matrices. This could be attributed to the restricted segmental mobility of PEGDA chains during a chain-growth network formation, as well as the low solid content of PEGDA in the initial feed composition.

3.3. Cytotoxicity Evaluation. The *In vitro* cytotoxicity testing using dermal fibroblasts was chosen to evaluate the

biocompatibility of the SS15PEG85 hydrogel sample. Results by the direct method demonstrate that hydrogels of pure PEGDA, SS15PEG85, and agar (5%) show no significant difference in cell viability of dermal fibroblasts both after 24 hr and 48 hr of incubation (Figure 8). More important results are found in the indirect method study, where the fibroblast cells were incubated in the PEGDA and SS18PEG85 extracts. At 24 hr and 48 hr of incubation, the dermal fibroblasts show increased cell viability comparing to the control cells ($p < 0.05$). The explanation could be related to the water-soluble PEGDA fragments that slowly diffuse out from the hydrogels during the extraction process. The loss of the gel fraction shown in Table 2 also provides evidence for this molecular diffusion. Likewise poly(ethylene glycol), PEGDA is believed to facilitate the membrane-stabilization effects to inhibit apoptotic cell death following injury [32–34]. The protective mechanism is still unclear. It could be attributed to the ability of PEGDA to form the thin film around the breached membrane and promote membrane rehealing. A protective film could also help to inhibit the mitochondrial swelling and so, suppress the production of reactive oxygen species (ROS). With the reduced apoptotic cell death, the production of the epidermal growth factor (EGF), acquired for the reepithelialization and granulation tissue formation in an early stage of wound healing, would be accelerated [35, 36]. This highlights the possibility of using the PEGDA-based hydrogels for the on-site delivery of the membrane healing agent, which would be advantageous for the treatment of chronic wounds. Regarding a balanced physicochemical and biocompatibility aspect, the SS15PEG85 has represented an ideal candidate for hydrogel wound dressing and tissue engineering matrices.

4. Conclusion

Silk semi-IPN hydrogels based on the PEDGA network were successfully prepared by radical polymerization. Results indicated that various hydrogel properties, including the gelation time, water content, sol fraction, and compressive strength, varied with the PEGDA content. As the amount of PEGDA was increased, the sol fraction and the silk gelation time were decreased. This illustrated a tightened network structure within the hydrogel matrices. At 15/85 (SS/PEGDA) mass percentage, the semi-IPN hydrogel showed the highest compressive properties, suggesting the strong impact of a balanced molecular interaction among SS, PEGDA, and water molecules within the system. More importantly, this 15/85 hydrogel showed excellent biocompatibility with no toxic effects towards the human dermal fibroblasts, thus representing a promising material for biomedical wound dressing in the future.

Data Availability

The data supporting the conclusions of this article are included within the article.

Conflicts of Interest

The authors declare that there is no conflict of interest regarding the publication of this paper.

Acknowledgments

This work was supported by the National Research Council of Thailand (NRCT) and Mae Fah Luang University.

References

[1] M. K. Sah and K. Pramanik, "Preparation, characterization and *in vitro* study of biocompatible fibroin hydrogel," *African Journal of Biotechnology*, vol. 10, no. 40, pp. 7878–7892, 2011.

[2] A. S. Hoffman, "Hydrogels for biomedical applications," *Advanced Drug Delivery Reviews*, vol. 54, no. 1, pp. 3–12, 2002.

[3] J. G. Hardy, L. M. Römer, and T. R. Scheibel, "Polymeric materials based on silk proteins," *Polymer*, vol. 49, no. 20, pp. 4309–4327, 2008.

[4] B. B. Mandal, A. S. Priya, and S. C. Kundu, "Novel silk sericin/-gelatin 3-d scaffolds and 2-d films: fabrication and characterization for potential tissue engineering applications," *Acta Biomaterialia*, vol. 5, no. 8, pp. 3007–3020, 2009.

[5] X. Wang, J. A. Kluge, G. G. Leisk, and D. L. Kaplan, "Sonication-induced gelation of silk fibroin for cell encapsulation," *Biomaterials*, vol. 29, no. 8, pp. 1054–1064, 2008.

[6] W. E. Hennink and C. F. van Nostrum, "Novel crosslinking methods to design hydrogels," *Advanced Drug Delivery Reviews*, vol. 54, no. 1, pp. 13–36, 2002.

[7] P. Chen, H. S. Kim, C.-Y. Park, H.-S. Kim, I.-J. Chin, and H.-J. Jin, "pH-triggered transition of silk fibroin from spherical micelles to nanofibrils in water," *Macromolecular Research*, vol. 16, no. 6, pp. 539–543, 2008.

[8] K. Thananukul, P. Jarruwale, N. Suttenun, P. Thordason, and P. Punyamoonwongsa, "Silk semi-interpenetrating network hydrogels for biomedical applications," *Macromolecular Symposia*, vol. 354, no. 1, pp. 251–257, 2015.

[9] D. Y. Ko, U. P. Shinde, B. Yeon, and B. Jeong, "Recent progress of in situ formed gels for biomedical applications," *Progress in Polymer Science*, vol. 38, no. 3-4, pp. 672–701, 2013.

[10] C. Yan and D. J. Pochan, "Rheological properties of peptide-based hydrogels for biomedical and other applications," *Chemical Society Reviews*, vol. 39, no. 9, pp. 3528–3540, 2010.

[11] M. Mondal, K. Trivedy, and S. N. Kumar, "The silk proteins, sericin and fibroin in silkworm, *Bombyx mori Linn*., a review," *Caspian Journal of Environmental Sciences*, vol. 5, pp. 63–76, 2007.

[12] A. Motta, C. Migliaresi, F. Faccioni, P. Torricelli, M. Fini, and R. Giardino, "Fibroin hydrogels for biomedical applications: preparation, characterization and in vitro cell culture studies," *Journal of Biomaterials Science, Polymer Edition*, vol. 15, no. 7, pp. 851–864, 2004.

[13] H. Tan and K. G. Marra, "Injectable biodegradable hydrogels for tissue engineering applications," *Materials*, vol. 3, no. 3, pp. 1746–1767, 2010.

[14] S.-Y. Xiong, Y.-D. Cheng, Y. Liu, S.-Q. Yan, Q. Zhang, and M.-Z. Li, "Effect of polyalcohol on the gelation time and gel structure of silk fibroin," *Journal of Biomedical Materials Research Part B*, vol. 3, pp. 236–243, 2011.

[15] B. B. Mandal, S. Kapoor, and S. C. Kundu, "Silk fibroin/polyacrylamide semi-interpenetrating network hydrogels for controlled drug release," *Biomaterials*, vol. 30, no. 14, pp. 2826–2836, 2009.

[16] D. Myung, D. Waters, M. Wiseman et al., "Progress in the development of interpenetrating polymer network hydrogels," *Polymers for Advanced Technologies*, vol. 19, no. 6, pp. 647–657, 2008.

[17] J. E. Leslie-Barbick, J. E. Saik, D. J. Gould, M. E. Dickinson, and J. L. West, "The promotion of microvasculature formation in poly(ethylene glycol) diacrylate hydrogels by an immobilized VEGF-mimetic peptide," *Biomaterials*, vol. 32, no. 25, pp. 5782–5789, 2011.

[18] X. Zhang, D. Yang, and J. Nie, "Chitosan/polyethylene glycol diacrylate films as potential wound dressing material," *International Journal of Biological Macromolecules*, vol. 43, no. 5, pp. 456–462, 2008.

[19] E. M. Merrill and E. W. Salzman, "Polyethylene oxide as a biomaterial," *ASAIO Journal*, vol. 6, no. 2, pp. 60–64, 1983.

[20] B. H. Cipriano, S. J. Banik, R. Sharma et al., "Superabsorbent hydrogels that are robust and highly stretchable," *Macromolecules*, vol. 47, no. 13, pp. 4445–4452, 2014.

[21] Deepa, A. K. T. Thulasidasan, R. J. Anto, J. J. Pillai, and V. Kumar, "Cross-linked acrylic hydrogel for the controlled delivery of hydrophobic drugs in cancer therapy," *International Journal of Nanomedicine*, vol. 7, pp. 4077–4088, 2012.

[22] M. Ghazinezhad, Y. V. Hryniuk, and L. P. Kru, "Preparation of hydrogels via cross-linking of partially hydrolyzed polyzcrylamides with potassium persulfate at moderate temeprature," *Der Chemica Sinica*, vol. 5, pp. 19–26, 2014.

[23] G. T. Gold, D. M. Varma, P. J. Taub, and S. B. Nicoll, "Development of crosslinked methylcellulose hydrogels for soft tissue augmentation using an ammonium persulfate-ascorbic acid redox system," *Carbohydrate Polymers*, vol. 134, pp. 497–507, 2015.

[24] E. Khor, H. Wu, L. Y. Lim, and C. M. Guo, "Chitin-methacrylate: preparation, characterization and hydrogel formation," *Materials*, vol. 4, no. 10, pp. 1728–1746, 2011.

[25] A. Matsumoto, J. Chen, A. L. Collette et al., "Mechanisms of silk fibroin sol-gel transitions," *Journal of Physical Chemistry B*, vol. 110, no. 43, pp. 21630–21638, 2006.

[26] W. Chen, Z. Wang, Z. Cui, D. Pan, and K. Millington, "Improving the photostability of silk using a covalently-bound UV absorber," *Polymer Degradation and Stability*, vol. 121, pp. 187–192, 2015.

[27] M. Nagura, R. Ohnishi, Y. Gitoh, and Y. Ohkoshi, "Structures and physical properties of cross-linked sericin membranes," *Journal of Insect Biotechnology and Sericology*, vol. 70, pp. 149–153, 2001.

[28] M. Tsukada, J. Magoshi, and K. Miyauchi, "Glass transition and crystallization of amorphous silk sericin," *Kobunshi Ronbunshu*, vol. 34, no. 1, pp. 71–73, 1977.

[29] S. Suzuki, R. Dawson, T. Chirila et al., "Treatment of silk fibroin with poly(ethylene glycol) for the enhancement of corneal epithelial cell growth," *Journal of Functional Biomaterials*, vol. 6, no. 2, pp. 345–366, 2015.

[30] C. Chen, T. Yao, S. Tu, W. Xu, Y. Han, and P. Zhou, "In situ microscopic studies on the structures and phase behaviors of SF/PEG films using solid-state NMR and Raman imaging," *Physical Chemistry Chemical Physics*, vol. 18, no. 24, pp. 16353–16360, 2016.

[31] Z. Zhang, Q. Li, C. Yesildag et al., "Influence of network structure on the crystallization behavior in chemically crosslinked hydrogels," *Polymers*, vol. 10, no. 9, p. 970, 2018.

[32] M. Bejaoui, E. Pantazi, M. Calvo et al., "Polyethylene glycol preconditioning: an effective strategy to prevent liver ischemia reperfusion injury," *Oxidative Medicine and Cellular Longevity*, vol. 2016, Article ID 9096549, 10 pages, 2016.

[33] R. Malhotra, V. Valuckaite, M. L. Staron et al., "High-molecular-weight polyethylene glycol protects cardiac myocytes from hypoxia- and reoxygenation-induced cell death and preserves ventricular function," *American Journal of Physiology-Heart and Circulatory Physiology*, vol. 300, no. 5, pp. H1733–H1742, 2011.

[34] J. Luo and R. Shi, "Polyethylene glycol inhibits apoptotic cell death following traumatic spinal cord injury," *Brain Research*, vol. 1155, pp. 10–16, 2007.

[35] M.-K. Yoo, H. Y. Kweon, K.-G. Lee, H.-C. Lee, and C.-S. Cho, "Preparation of semi-interpenetrating polymer networks composed of silk fibroin and poloxamer macromer," *International Journal of Biological Macromolecules*, vol. 34, no. 4, pp. 263–270, 2004.

[36] S. Werner and R. Grose, "Regulation of wound healing by growth factors and cytokines," *Physiological Reviews*, vol. 83, no. 3, pp. 835–870, 2003.